200 Gb/s Wireless Transmission Using Dual-Polarized OAM-MIMO Multiplexing With Uniform Circular Array on 28 GHz Band

Yasunori Yagi, *Member, IEEE*, Hirofumi Sasaki, *Member, IEEE*, Takayuki Yamada, *Member, IEEE*, and Doohwan Lee, *Member, IEEE*

***Abstract*—In this letter, we present a dual-polarized orbital angular momentum multiple-input.multiple-output (OAM-MIMO) with uniform circular arrays (UCAs) that achieves a transmission rate of over 200 Gb/s. We design and evaluate the properties of microstrip antennas on 28 GHz band and then fabricate the antennas and implement them on a transmitter and receiver with four UCAs disposed concentrically. Each UCA consists of 16 microstrip antenna elements and is connected to a Butler matrix that can generate and separate five OAM modes (±2, ±1, and 0). There is also a center antenna capable of transmitting mode 0, so the total number of antenna elements is 65 and 21 streams can be transmitted simultaneously. In order to maximize the transmission capacity, we use polarization multiplexing. We conduct two data transmission experiments at a distance of 10 m. In the experiment of virtual dual-polarized OAM-MIMO transmission, we achieved approximately 110 Gb/s transmission for both polarizations. In the experiment of 21 streams, simultaneous transmission of dual-polarized OAM-MIMO, the result of 201.5 Gb/s was achieved.**

***Index Terms*—Microstrip antennas, orbital angular momentum multiple-input.multiple-output (OAM-MIMO), polarization, uniform circular array (UCA).**

I. Introduction

THE demand for high-capacity wireless transmission is increasing due to increasing data traffic. The use of spatial multiplexing technologies such as multiple-input–multiple-output (MIMO) [1] is one of the most effective approaches for increasing the capacity of wireless transmissions; in 5G networks and beyond, the development of millimeter-wave technology makes it possible to achieve high-capacity wireless transmissions [2]. In this network, point-to-point wireless transmission becomes very important in terms of mobile backhaul and fronthaul.

Orbital angular momentum (OAM) multiplexing is of interest in point-to-point wireless transmission systems [3]–[7]. The wavefront phase of an electromagnetic (EM) wave with OAM mode l varies from 0 to $2\pi k$. This phase rotation is known as "OAM modes" ($l = 0, \pm1, \pm2, \pm3, \ldots$), where the modes are spatially orthogonal and allow for the multiplexing of different OAM modes. Several studies have been conducted on OAM multiplexing for high-capacity wireless and free-space optical data transmission [8]–[13]. Yan *et al.* [13] demonstrated 32 Gb/s, 60 GHz wireless transmission using a spiral phase plate (SPP). An SPP can convert a plane wave into an OAM beam, and by changing the shape of the SPP, different OAM modes can be generated and then combined using a beam combiner. Another way to generate OAM modes is to use a uniform circular array (UCA) [14]. Multiplexed OAM modes can be emitted from a single UCA by providing the antenna element with a combined radio frequency (RF) signal of multiple OAM modes. To achieve high spectral efficiency, a combination of OAM and MIMO, polarization, or both is an effective approach. Therefore, a microstrip antenna is required for achieving dual-polarized OAM-MIMO multiplexing transmission with multi-UCA. In this letter, we design and fabricate a microstrip antenna that has a gain of over 11 dBi. We also implement OAM-MIMO multiplexing equipment and use it to perform data transmission experiments.

In Section II, we discuss OAM multiplexing using UCA. In Section III, we present our design and fabrication of the microstrip antenna for UCA and evaluate the radiation pattern and gain. In Section IV, we discuss our implementation of an end-to-end wireless OAM-MIMO transmission system and report the results of two wireless data transmission experiments using dual-polarized OAM-MIMO multiplexing.

II. OAM Multiplexing Using UCA

An OAM beam is formed by applying a certain phase gradient to the antenna elements of a UCA. OAM mode l is generated by giving the phase gradient $\varphi = 2\pi l/n$, where n is the number of antenna elements. One approach to generating an OAM multiplexed beam is to use the Butler matrix, which is an analog circuit that performs discrete Fourier transform (DFT) processing. When the transmitter (Tx) UCA and receiver (Rx) UCA are coaxial on opposite sides of the propagation direction, and the number of antennas is the same in both sides, the channel matrix $\boldsymbol{H}$ becomes a circulant matrix [15]

$$\boldsymbol{H} = \boldsymbol{V}_n \boldsymbol{\Sigma} \boldsymbol{V}_n^H \tag{1}$$

where $\boldsymbol{V_n}$ is an $n \times n$ DFT matrix, $\boldsymbol{V}_n^H$ is a Hermitian conjugate of $\boldsymbol{V_n}$, and Σ is a diagonal matrix with independent components for each OAM mode. Equation (1) holds true for isotropic antenna while slight deviation might exist when microstrip antenna in the

Manuscript received November 19, 2020; revised December 28, 2020, February 3, 2021, and March 4, 2021; accepted March 4, 2021. Date of publication March 11, 2021; date of current version May 5, 2021. *(Corresponding author: Yasunori Yagi.)*

The authors are with the NTT Network Innovation Laboratories, NTT Corporation, Yokosuka 239-0847, Japan (e-mail: yasunori.yagi.zc@hco.ntt.co.jp; hirofumi.sasaki.uw@hco.ntt.co.jp; takayuki.yamada.zb@hco.ntt.co.jp; doohwan.lee.yr@hco.ntt.co.jp).

Digital Object Identifier 10.1109/LAWP.2021.3065098

UCA has a directional gain. However, we confirmed that such deviation is negligible in the considered experimental environment as described in the following chapter. Therefore, this antenna element can be regarded as isotropic at the Rx antenna. Next, we consider extending OAM to OAM-MIMO with multi-UCAs. By placing multiple UCAs coaxially, the equivalent channel matrix $\mathbf{\Lambda}$ including DFT processing on Tx and Rx becomes a block diagonal matrix as

$$\mathbf{\Lambda}' = \begin{bmatrix} \mathbf{\Lambda}_{l_{(1)}} & & \boldsymbol{O} \\ & \ddots & \\ \boldsymbol{O} & & \mathbf{\Lambda}_{l_{(m)}} \end{bmatrix} \tag{2}$$

where Λ' is a block diagonal matrix of OAM mode *l(m)* [16], and *m* is the index of the OAM mode. While each $\Lambda_{l(m)}$ is separated by a Butler matrix, each element of $\Lambda_{l(m)}$ is a channel with the same mode transmitted from different UCAs so it is separated by MIMO equalization [17]. Hence, the number of multiplexes can be increased by separating the channels between UCAs by MIMO equalization while maintaining the orthogonality of each mode.

III. Microstrip Antenna for Uniform Circular Array

A. Antenna Design

Our objective in this work is to achieve over 200 Gb/s transmission by OAM-MIMO multiplexing using a 27.5–29.5 GHz band at a distance of 10 m. In this letter, we set the required signal-to-noise ratio (SNR) is more than 15 dB for the error-free transmission with the usage of the channel coding. The receiving SNR of each mode is given by

$$\mathrm{SNR} = P_T + G_T - P_L + G_R - P_N + NF \tag{3}$$

where P_T, G_T, P_L, G_R, P_N, and *NF* are respectively Tx power, Tx antenna gain, path loss, Rx antenna gain, thermal noise, and noise figure. In the case of UCA-based OAM transmission, P_L takes the following unique values [18]:

$$P_L = \left| \sum_{n=0}^{N_r-1} \sum_{m=0}^{N_t-1} \frac{1}{\sqrt{N_r N_t}} \exp\left(j2\pi l\left(\frac{m}{N_t} - \frac{n}{N_r}\right) - jkr_{mn}\right) \frac{\lambda}{4\pi r_{mn}} \right|^2 \tag{4}$$

where N_t, N_r, k, l, λ, and r_{mn} are respectively the number of Tx antenna elements, the number of Rx antenna elements, wavenumber, OAM mode, wavelength, and the distance from element *m* of the Tx to element *n* of the Rx. In this work, these are set as follows considering the experimental environment: $P_T = 0$ dBm, $P_N = -81$ dBm, and $NF = 6$ dB. In particular, P_L is set from 63 to 83 dB because it varies on the parameters of N_t, N_r, l, λ, and r_{mn}. To obtain a SNR of 15 dB or higher under the highest path loss condition of which value is 83 dB [19], the summation of Tx and Rx antenna gains must be equal or higher than 22 dBi, i.e., $G_T + G_R \geq 22$ dBi. Hence, we set a target of designing antennas with more than 11 dBi. Microstrip antennas with a gain of more than 11 dBi have been proposed in a narrow 5 GHz band [20]. There have also been reports of small microstrip antennas with a wide bandwidth of less than 11 dBi for the millimeter-wave band [21]–[23]. We therefore designed 27.5–29.5 GHz microstrip antennas with the gain of over 11 dBi. Fig. 1 shows the multi-UCAs for OAM-MIMO multiplexing, where four UCAs are disposed concentrically. Each UCA has 16 antenna elements, with an additional one in the center, so the Tx has a total of 65 antenna elements. The layer configuration of the patch antenna elements is shown in Fig. 2. This antenna element has four layers consisting of a parasitic element, an excitation element, GND, and a feedline from the top. The parasitic element consists of seven elements to obtain a directional gain. Each element is spaced at intervals of 5.2 mm, which is half a wavelength at the center frequency of 28.5 GHz.

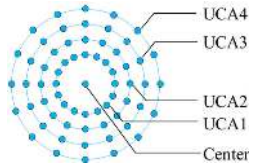

Fig. 1. OAM-MIMO multiplexing with four UCAs and center antenna.

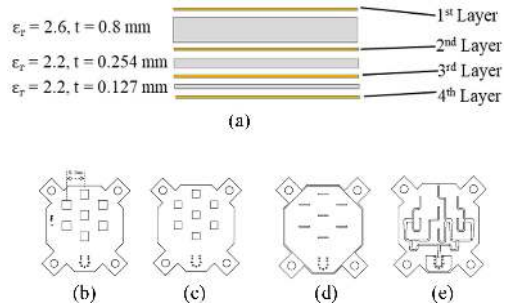

Fig. 2. Layer pattern. (a) Layer structure. (b) First layer. (c) Second layer. (d) Third layer. (e) Fourth layer.

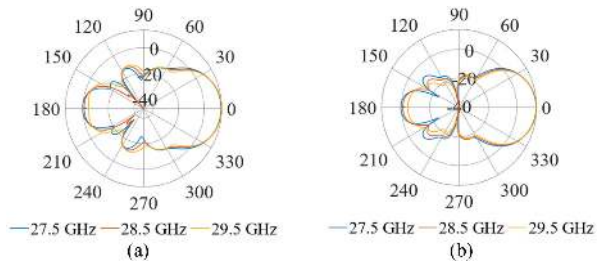

Fig. 3. Radiation pattern simulation. (a) Vertical plane. (b) Horizontal plane.

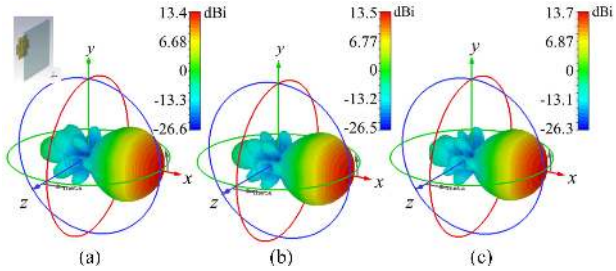

Fig. 4. 3-D radiation pattern. (a) 27.5, (b) 28.5, and (c) 29.5 GHz.

B. Antenna Radiation Pattern and Gain Evaluation

First, we calculated the directivity gain in the horizontal (H) and vertical (V) planes of the antenna elements using an EM wave simulator. The radiation patterns are shown in Fig. 3. The front directional directivity in both the vertical and horizontal planes was over 11 dBi. The 3-D radiation pattern is shown in Fig. 4.

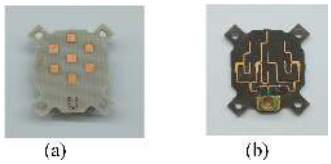

Fig. 5. Fabricated patch antenna (a) front and (b) back.

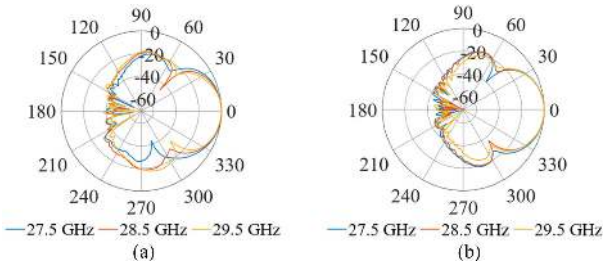

Fig. 6. Antenna radiation pattern measurements. (a) Vertical plane. (b) Horizontal plane.

TABLE I
AVERAGE ANTENNA GAIN OF 130 ELEMENTS

27.5 GHz	28.5 GHz	29.5 GHz
11.3 dBi	12.0 dBi	12.0 dBi

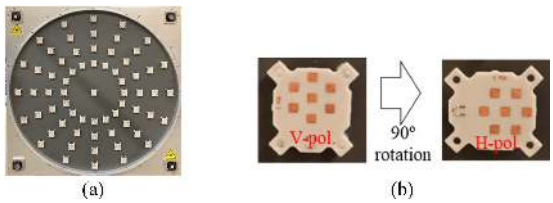

Fig. 7. (a) OAM-MIMO multiplexing equipment with four UCAs and center antenna. (b) Patch antenna element with V-polarization and H-polarization.

Next, we fabricated the antenna elements shown in Fig. 5. The antenna element was connected to the Tx and Rx via a sub miniature push-on (SMP) connector. The measurements of the radiation pattern in the horizontal and vertical planes of the antenna elements are shown in Fig. 6. The amplitudes were normalized to be 0 dB in the frontal direction and we measured at frequencies of 27.5, 28.5, and 29.5 GHz. In each frequency and both radiation patterns, the side lobes were approximately less than −20 dB. Then, we fabricated all antenna elements to attach to the Tx and Rx UCAs and measured the gains. The antenna gain is shown in Table I. The average gain at the center frequency (28.5 GHz) was 12.0 dBi. The deviation between all the elements was limited to 0.9 dB, which is allowable for OAM transmission at a distance of 10 m.

IV. TRANSMISSION EXPERIMENTS

We implemented a 28 GHz band OAM-MIMO transmission equipment using the microstrip antennas shown in Fig. 7(a). This antenna element has V polarization, so different polarized EM waves can be generated by rotating each antenna element 90 degrees, as shown in Fig. 7(b). We conducted two experiments on this equipment with different approaches for the polarization multiplexing: 1) virtual 22 stream transmission and 2) 21 stream simultaneous transmission. In both experiments, we set up the OAM-MIMO communication link shown in Fig. 8. We applied two Gbaud digital intermediate frequency (IF) signals to three arbitrary waveform generators (AWG). The AWGs output analog IF signals to the Tx, and these were then upconverted to the RF frequency in the Tx. Finally, OAM multiplexing signals were generated by Butler matrices for each UCA and then transmitted. We designed the Butler matrix to achieve more than 15 dB of mode isolation, which is required for 100 Gb/s transmission including forward-error correction (FEC). The transmitted signals were received by the Rx located ten meters away (shown in Fig. 9), and the digital serial analyzer (DSA) stored the received IF signals that were separated for each mode by processing opposite the Tx. The saved data were demodulated by offline digital signal processing. We used adaptive modulation and coding (AMC) to select the appropriate modulation and coding rate depending on the SNR. Then, we evaluated the transmission capacity where the number of error bits became zero with FEC. Table II shows the experimental parameters.

TABLE II
EXPERIMENTAL PARAMETERS

Parameters	Values
Frequency	27.5–29.5 GHz
OAM modes	−2, −1, 0, 1, 2
Diameter of UCAs	24, 36, 48, 60 cm
FEC (Outer/Inner)	BCH/LDPC
Equalization	SC-FDE/MMSE
Modulation (prepared)	QPSK–256QAM
Coding rate (prepared)	1/2, 3/5, 2/3, 3/4, 4/5, 5/6, 8/9, 9/10

First, we evaluated the cross-polarization interference. Fig. 10 shows the spectrum of the received IF signal when the modulated signal was transmitted. The solid blue line indicates the received signal power of the same polarization for Tx and Rx, and the dotted red line indicates the received signal power of different polarizations. The maximum power values were normalized to 0 dB. The difference between the power of the same polarization and the power of the different polarizations indicates cross-polarization interference. This interference was attenuated to approximately −25 dB, which demonstrates that the cross-polarization interference is negligible.

A. Experiments on Virtual Dual-Polarized OAM-MIMO Transmission

In this experiment, the data were transmitted for each polarization and the transmission rate was compared. In order to maximize the transmission rate, we utilized UCA 1, UCA 4, and the center antenna, so the total number of streams was 11. Rx chose all the UCAs to obtain Rx diversity. This configuration was the same as [17]. First, the signals were transmitted with both the Tx and Rx UCAs in V polarization. In other words, the signals were copolarized. Next, the signals were transmitted from the Tx UCAs in the H-polarization and were received by the Rx UCAs in the V- polarization. We combined both waveforms during signal processing in order to evaluate the demodulated transmission rate of the signal containing polarization interference. The V- and H-polarization transmission capacity of 11 streams reached 109.8 and 111.67 Gb/s, respectively, so we considered there was little difference between the two. The slight difference in the capacities was due to the quantization of the SNRs when we applied AMC. According to these results, we can achieve over

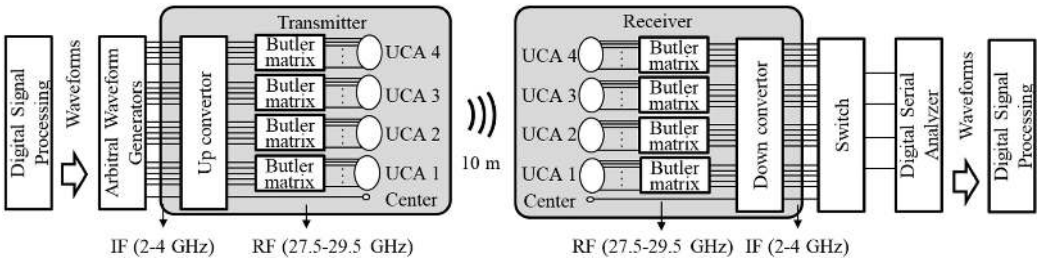

Fig. 8. Diagram of OAM-MIMO communication link.

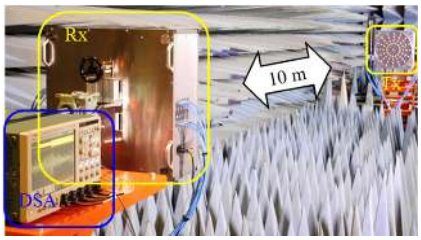

Fig. 9. Experimental environment in shielded room.

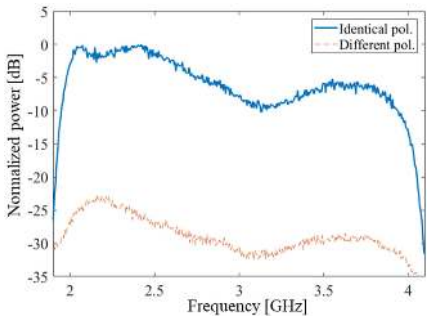

Fig. 10. Spectrum of received IF waveform of UCA 1, mode +2. The value of maximum power in the signal band (2–4 GHz) is normalized to 0 dB.

220 Gb/s transmission if we implement dual-polarized UCAs and RF chains. This can be easily accomplished by arranging the patch antennas of each polarization alternately on the same circumference.

B. Experiment on 21-Stream Simultaneous Dual-Polarized OAM-MIMO Transmission

Our implemented OAM-MIMO equipment should select V- or H-polarizations in each UCA. UCA 1 and UCA 3 were H-polarization, and UCA 2, UCA 4, and the center antenna were V polarization. This was the same for both the Tx and Rx UCAs. The total streams were 21 signals, which was the maximum streams of simultaneous transmission in this equipment. We selected polarizations alternately to reduce the correlation between UCAs that had the same polarization. Crosstalk between different polarizations was low enough that no signal processing was applied to reduce cross-polarization interference. Table III shows the resulting transmission rates, modulations, and coding rates. Each stream achieved 4.0 to 13.3 Gb/s transmission using 16QAM, 1/2 to 256QAM, 5/6 modulations, and coding rates. The sum of the 10 stream transmission capacities of UCA 1 and 3 with H-polarization was 81.2 Gb/s. That of UCA 2 and 4 with V-polarization was 110.2 Gb/s. The capacity of the V-polarized UCA was more than that of the H-polarized UCA because the UCA radii of the V-polarized UCA and H-polarized UCA were different. The remaining capacity of the V-polarized center antenna was 10.0 Gb/s. As a result, the total capacity of 21 streams reached 201.5 Gb/s. We achieved 100.75 b/s/Hz spectral efficiency.

TABLE III
TRANSMISSION RATE AND USED MODULATION AND CODING FOR EACH STREAM OF 201.5 Gb/s TRANSMISSION

OAM mode		Center	UCA 1	UCA 2	UCA 3	UCA 4
	Parameters	V pol.	H pol.	V pol.	H pol.	V pol.
−2	Modulation		16QAM	256QAM	16QAM	64QAM
	Coding rate		1/2	5/6	5/6	5/6
	Rate [Gbit/s]		4.0	13.3	6.7	10.0
−1	Modulation		64QAM	256QAM	64QAM	64QAM
	Coding rate		4/5	3/4	4/5	5/6
	Rate [Gbit/s]		9.6	12.0	9.6	10.0
0	Modulation	64QAM	256QAM	64QAM	64QAM	64QAM
	Coding rate	5/6	3/4	5/6	4/5	5/6
	Rate [Gbit/s]	10.0	12.0	10.0	9.6	10.0
1	Modulation		256QAM	64QAM	64QAM	64QAM
	Coding rate		3/4	9/10	3/5	5/6
	Rate [Gbit/s]		12.0	10.8	7.2	10.0
2	Modulation		16QAM	256QAM	16QAM	64QAM
	Coding rate		2/3	5/6	4/5	9/10
	Rate [Gbit/s]		5.3	13.3	6.4	10.8

Total capacity: 201.5 Gb/s.

V. CONCLUSION

In this letter, we have demonstrated over 200 Gb/s transmission using OAM-MIMO multiplexing with multi-UCAs on a 28 GHz band. We first designed and fabricated microstrip antennas for dual-polarized OAM-MIMO transmission using multi-UCAs. The antenna gain was over 11 dBi and could transmit OAM signals 10 m away. Then, we implemented dual-polarized OAM-MIMO transmission equipment composed of four UCAs. Each UCA could multiplex five OAM modes (± 2, ± 1, and 0) and transmit V- or H-polarization. Finally, we reported the results of two data transmission experiments using dual-polarized OAM-MIMO multiplexing in a shielded room at a distance of 10 m. In the experiment of virtual dual-polarized OAM-MIMO transmission, 109.8 and 111.67 Gb/s transmission was achieved with V- and H-polarizations, respectively. In the experiment of simultaneous dual-polarized OAM-MIMO transmission, 201.5 Gb/s transmission was achieved, which is a remarkable result on a 28 GHz band.

REFERENCES

[1] D. Gesbert, M. Shafi, D. Shiu, P. J. Smith, and A. Naguib, "From theory to practice: An overview of MIMO space-time coded wireless systems," *IEEE J. Sel. Areas Commun.*, vol. 21, no. 3, pp. 281–302, Apr. 2003.

[2] I. Parvez, A. Rahmati, I. Guvenc, A. I. Sarwat, and H. Dai, "A survey on low latency towards 5G: RAN, core network and caching solutions," *Commun. Surveys Tuts.*, vol. 20, no. 4, pp. 3098–3130, May 2018.

[3] L. Cheng, W. Hong, and Z. Hao, "Generation of electromagnetic waves with arbitrary orbital angular momentum modes," *Sci. Rep.,* vol. 4, pp. 4814–4818, Apr. 2014.

[4] K. Murata, N. Honma, K. Nishimori, N. Michishita, and H. Morishita, "Analog eigenmode transmission for short-range MIMO based on orbital angular momentum," *IEEE Trans. Antennas Propag.*, vol. 65, no. 12, pp. 6687–6702, Dec. 2017.

[5] D. Lee, H. Sasaki, H. Fukumoto, K. Hiraga, and T. Nakagawa, "Orbital angular momentum (OAM) multiplexing: An enabler of a new era of wireless communications," *IEICE Trans. Commun.*, vol. E100-B, no. 7, pp. 1044–1063, Jul. 2017.

[6] S. M. Mohammadi *et al.*, "Orbital Angular momentum in radio—A system study," *IEEE Trans. Antennas Propag.*, vol. 58, no. 2, pp. 565–572, Feb. 2010.

[7] T. Yuan, Y. Cheng, H. Wang, and Y. Qin, "Mode characteristics of vortical radio wave generated by circular phased array: Theoretical and experimental results," *IEEE Trans. Antennas Propag.*, vol. 65, no. 2, pp. 688–695, Feb. 2017.

[8] J. Wang *et al.*, "Experimental demonstration of free-space optical communications using OFDM-QPSK/16QAM-carrying fractional orbital angular momentum (OAM) multiplexing," in *Proc. Opt. Fiber Commun. Conf.*, Mar. 2015, pp. 1–3.

[9] P. Martelli, A. Gatto, P. Boffi, and M. Martinelli, "Free-space optical transmission with orbital angular momentum division multiplexing," *Electron. Lett.*, vol. 47, no. 17, pp. 972–973, Aug. 2011.

[10] Y. Yan *et al.*, "High-capacity millimeter-wave communications with orbital angular momentum multiplexing," *Nature Commun.*, vol. 5, Sep. 2014, Art. no. 4876.

[11] C. Xu *et al.*, "Free-space radio communication employing OAM multiplexing based on Rotman lens," *IEEE Microw. Wireless Compon. Lett.*, vol. 26, no. 9, pp. 738–740, Sep. 2016.

[12] D. Lee *et al.*, "An experimental demonstration of 28 GHz band wireless OAM-MIMO (orbital angular momentum multi-input and multi-output) multiplexing," in *Proc. IEEE 87th Veh. Technol. Conf.*, Jun. 2018, pp. 1–5.

[13] Y. Yan *et al.*, "32-Gbit/s 60-GHz millimeter-wave wireless communication using orbital angular momentum and polarization multiplexing," in *Proc. IEEE Int. Conf. Commun.*, May 2016, pp. 1–6.

[14] R. Chen, H. Zhou, M. Moretti, X. Wang, and J. Li, "Orbital angular momentum waves: Generation, detection, and emerging applications," *IEEE Commun. Surveys Tuts.*, vol. 22, no. 2, pp. 840–868, Nov. 2019.

[15] R. Chen, H. Xu, M. Moretti, and J. Li, "Beam steering for the misalignment in UCA-based OAM communication systems," *IEEE Wireless Commun. Lett.*, vol. 7, no. 4, pp. 582–585, Aug. 2018.

[16] Y. Yagi, H. Sasaki, T. Yamada, and D. Lee, "200 Gbit/s wireless transmission using dual-polarized OAM-MIMO multiplexing on 28 GHz band," in *Proc. IEEE GLOBECOM workshop*, Dec. 2019, pp. 1–4.

[17] H. Sasaki *et al.*, "Experiment on over-100-Gbps wireless transmission with OAM-MIMO multiplexing system in 28 GHz band," in *Proc. IEEE GLOBECOM*, Dec. 2018, pp. 1–6.

[18] D. Nguyen *et al.*, "Discussion about the link budget for electromagnetic wave with orbital angular momentum," in *Proc. 8th Eur. Conf. Antennas Propag.*, Apr. 2014, pp. 1117–1120

[19] H. Sasaki, Y. Yagi, T. Yamada, and D. Lee, "Field experimental demonstration on OAM-MIMO wireless transmission on 28 GHz band," in *Proc. IEEE GLOBECOM Workshop*, Dec. 2019, pp. 1–4.

[20] H. Lui, L. Kang, F. Wei, Y. Cai, and Y. Yin, "A low-profile dual-polarized microstrip antenna array for dual-mode OAM applications," *IEEE Antennas Wireless Propag. Lett.*, vol. 16, pp. 3022–3025, 2017.

[21] M. Magray, G. S. Karthikeya, K. Muzaffar, S. Koul, and A. Moon, "Wideband asymmetric coplanar strip fed antennas with pattern diversity for mmWave 5G base stations," *IEEE Access,* vol. 8, pp. 77482–77489, 2020.

[22] H. Chen, Y. Shao, Y. Zhang, C. Zhang, and Z. Zhang, "A low-profile broadband circularly polarized mm wave antenna with special-shaped ring slot," *IEEE Antennas Wireless Propag. Lett.*, vol. 18, no. 7, pp. 1492–1496, Jul. 2019.

[23] J. Yin, Q. Wu, C. Yu, H. Wang, and W. Hong, "Broadband symmetrical E-shaped patch antenna with multimode resonance for 5G millimeter-wave applications," *IEEE Trans. Antennas Propag.*, vol. 67, no. 7, pp. 4474–4483, Jul. 2019.